Combustion joining of refractory materials: Carbon–carbon composites

Jeremiah D.E. White
Department of Chemical and Biomolecular Engineering, University of Notre Dame, Notre Dame, Indiana 46556

Allen H. Simpson
Honeywell Aerospace, South Bend, Indiana 46628

Alexander S. Shteinberg
ALOFT, Berkeley, California 94708

Alexander S. Mukasyan[a)]
Department of Chemical and Biomolecular Engineering, University of Notre Dame, Notre Dame, Indiana 46556

(Received 18 July 2007; accepted 20 September 2007)

Refractory materials such as carbon possess properties that make joining them difficult. In this work, bonding of a carbon–carbon composite is achieved by employing self-sustained, oxygen-free, high-temperature combustion reactions. The effects of several parameters, such as the composition of the reaction media, and the values of the applied current and pressure, on the mechanical strength of the joint were investigated. It was found that the C–C composite possesses a high activity with the reactive media layer, the level of electrical current used to initiate the reaction and the applied pressure do not need to be excessive to obtain a strong joint. Some aspects of the joining mechanism are discussed in detail.

I. INTRODUCTION

Carbon–carbon (C–C) composites have low density and a high strength-to-weight-ratio, and are able to withstand high temperatures. This combination of properties makes C–C composites well suited for a variety of applications including turbine engine components, the nosecone and leading edges of the wings of space shuttles,[1] and carbon brakes.[2] As the number of relevant applications for such materials increase, technology for joining the C–C components will need to be developed to produce a wider variety of sizes and geometries. More specifically, an effective bonding method would be of great benefit to existing industries that manufacture C–C components, such as Honeywell Aerospace (South Bend, IN).[3] For example, through C–C joining, Honeywell Aerospace could perform a refurbishment of the carbon brakes by bonding a new thin C–C element to a used "core" to produce a brake that meets the performance specifications. The combustion-joining (CJ) method, which will be described further, is an attractive approach for bonding refractory materials. Advances in materials joining using combustion phenomena have been discussed in detail in a recent review.[4]

Selecting an appropriate joining method is dictated not only by the material, but also by the geometry of and intended use for the finished part. Example techniques include mechanical means (e.g., screws, nails, and bolts), adhesives (e.g., glues and epoxies), soldering, and welding. Welding is typically reserved for use with metals, and even refractory compositions (i.e., those with high melting temperature) can be welded if enough control is exercised over the welding conditions. However, joining C–C composites is not a simple task. Mechanical or adhesive means could be used with such materials, but the application would be severely limited. For example, in the case of the carbon-brake application, which demands highly refractory components, traditional mechanical or adhesive joining would not hold up to the harsh environment. Unlike metals, they do not lend themselves to welding, and even brazing can be difficult because many filler metals that are commonly used exhibit little or no wetting with carbon materials. Even with suitable filler metal, brazing normally requires special surface treatment, adding to the time and cost of joining. Thus, it is not surprising that there are only a few studies specifically concerning the bonding of C–C composites with a refractory layer.[5–9]

Because carbon is a very refractory element and cannot be welded, it would be desirable to form a chemically bonded joint that exhibits a thermal expansion and

[a)]Address all correspondence to this author.
e-mail: amoukasi@nd.edu
DOI: 10.1557/JMR.2008.0008

resistance similar to those of the bulk carbon. A few studies involving C–C composites specifically have used various layer compositions including refractory borides (TiB_2 and ZrB_2),[7] carbides (SiC, B_4C, and WC),[6–9] or their mixtures (TiB_2 + SiC + B_4C),[7] relying on the solid-state diffusion bonding mechanism. Though relatively strong bonding is achieved, this method suffers from distinct shortcomings. It requires long (hours), high-temperature (~2000 K) sample treatment under relatively high loads. These conditions are imposed by the physical nature of solid-state reactions, which are generally slow. Also, solid media require the application of a high load to obtain a pore-free layer and, thus, a good joint. Furthermore, a long heat treatment at high temperatures could detrimentally affect the properties of the C–C composite itself. All of these disadvantages can be overcome if joining is conducted with the involvement of a liquid phase. Unfortunately, the melting points of the desired refractory phases (e.g., TiB_2, TiC, and WC) are very high (~3000 K) and thus not attainable in conventional large-scale furnaces. However, such temperatures can easily be obtained through the combustion of exothermic reaction mixtures.

The development of an approach called self-propagating high-temperature synthesis (SHS), or combustion synthesis (CS),[10–12] significantly expanded the class of exothermic reactions that can be used to produce materials. Briefly, this method is characterized by the propagation of a high-temperature combustion reaction after the local ignition of a heterogeneous exothermic mixture. In the self-propagating mode, the reaction front moves rapidly in a self-sustained manner leading to the formation of the final solid products without the need for any additional energy. In the volume CS (VCS) mode, the entire sample is heated uniformly in a controlled manner until the reaction ignites throughout its volume.

While initially developed for the synthesis of materials and powders, this approach is attracting more and more attention as a tool for joining various substances, which is hereafter referred to as CJ. Several CJ schemes for the bonding of different materials, including superalloys, refractory metals (e.g., Mo and Ta), and ceramics, have been reported.[12–21] A classification scheme for such CJ approaches suggested in the study by Mukasyan and White[4] is shown in Fig. 1. First, similar to the material synthesis case, these methods can be divided into SHS and VCS joining. In the first scheme, the reaction is locally (in a spot volume of several hundreds of microns) initiated (e.g., by means of a laser or electrically heated metal wire) in the reaction layer, and a self-sustained combustion wave propagates along the reactive media, leading to a high-temperature interaction between the layer and the chemically "welded" pieces. The second scheme assumes that the reactive layer is externally preheated to its so-called self-ignition temperature, and thus the reaction is initiated uniformly throughout the entire volume of the layer.

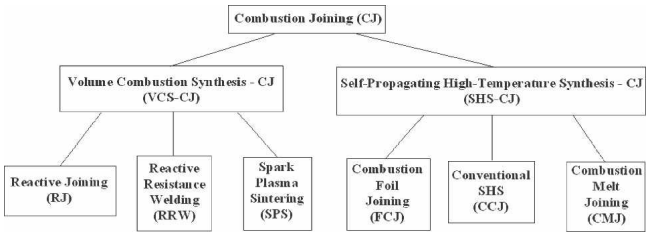

FIG. 1. Classification scheme for CJ methods.

In this work, we further developed the so-called reactive resistance-welding (RRW) method,[14,19,20,22] which falls under the volume combustion joining category. Note that another technique that uses a similar schematic is the spark plasma-sintering (SPS) method.[23] An important distinction, however, is that in SPS electrical current is important to promote the reaction-sintering process, while in the case of RRW it is used only to preheat the stack and uniformly initiate a reaction. Moreover, for many materials it is undesirable to keep electrical current flowing for a long time, because it may lead to degradation in their properties.

II. EXPERIMENTAL

The approach used in this work for joining C–C composites used the concept of self-sustained, oxygen-free, high-temperature reactions in heterogeneous mixtures. Such reactive mixtures typically consist of metal and nonmetal powders mixed in a desired ratio (e.g., Ti + C or Ti + B). A detailed discussion of the apparatus designed and used for our application can be found elsewhere.[22] Briefly, referring to Fig. 2, a layer of reactive mixture (1) is contained between two disks of the C–C composite (2) that are to be joined. The stack (1, 2) is

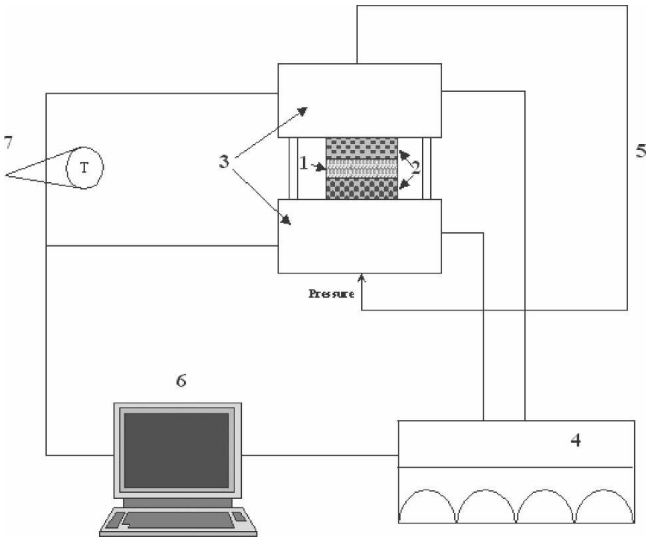

FIG. 2. Schematic diagram of the RRW joining process.

held in place between two electrodes (3), which are connected to a direct current (dc) power supply (4). The dc current is used to preheat the stack and uniformly initiate the reaction in the reactive layer. Note that because the resistivity of the porous powder media is higher than that of the composite, Joule heat is primarily evolved in this thin layer. The electrodes are also part of the pneumatic system (5), which applies a load to the stack. All operational parameters such as initial pressure (P_i) and final pressure (P_f), applied current (I_{max}), delay time between ignition and final pressure application (Δt_l), duration of Joule heating (Δt_h), and others are defined by a programmable logic controller (6) system.

Once the mixture has reached ignition temperature (T_{ig}), the reaction proceeds rapidly (seconds) in a self-sustained manner reaching a maximum temperature (T_m) on the order of 3000 K. The temperature of the stack can be sensed with a thermocouple or an optical system (7). After a predetermined Δt_l, the pressure applied to the stack is increased to promote interaction between the hot reactive mixture and the C–C layers. The process-temperature profile measured using a pyrometer, shown in Fig. 3, confirms that the temperature rapidly increases, initiating the reaction. In a short period of time (<5 s), the reactive layer was heated to a temperature sufficient to initiate the reaction. Also of note is that heat builds up in the reactive layer faster than in the C–C composite, as expected. After allowing the stack to cool for a few minutes, it was removed from the die and the C–C composites were joined together.

All samples were prepared using C–C composite cylinders (Honeywell, South Bend, IN) with D = 10 mm, l_c = 25 mm because characterization work, such as microstructure and strength measurements, is easy to perform in them. Different powders, including Ti (<149 μm), B (<5 μm), and Ni (<48 μm) from Alfa Aesar, (Ward Hill, MA) C (~0.068 μm) from Fisher Scientific (Fair Lawn, NJ), and 25-μm Ti foil from Alfa Aesar were used to make reactive-bonding media. For reactive layers consisting of powders, the desired composition was mixed together and then pressed into a die (D = 10 mm) using 57 MPa of pressure. In all experiments discussed in this article, the initial pressure applied to the joining stack was P_i = 3.5 MPa, which was then increased to the desired level (P_f) at Δt_l = 1.0 s after beginning Joule preheating; the application of the current was terminated at Δt_h = 5.0 s. When determining the dependency of joint strength based on the current used to initiate the combustion reaction (600, 700, and 800 A), P_f was 51 MPa. In determining the dependency of strength based on the applied pressure, 600 A of current was used, and the P_f was varied from 3.5 to 51 MPa. To quantify the quality of the obtained joints under various conditions, mechanical testing of the joined samples was performed using a tensile load on a universal testing machine (Series 900; Applied Test Systems, Butler, PA). Each sample was loaded into a pair of friction grips (Applied Test Systems), with the joint spaced equally between the contact points of each grip. The tensile load required to break the sample was then used to calculate the pressure that was placed on the joining area. The joint microstructure and phase composition were also characterized using a scanning electron microscope (EVO 50 Series; Zeiss, Peabody, MA) and electron dispersive spectroscopy analysis (INCAx-sight Model 7636; Oxford Instruments, Concord, MA).

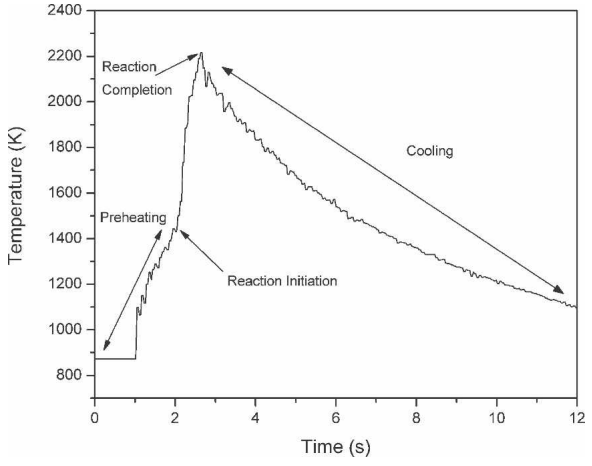

FIG. 3. Typical temperature–time profile of the RRW joining process.

The effect of several parameters on the mechanical properties and microstructure of the produced joint have been investigated (i.e., the influence of reactive layer composition, the magnitude of the current used for preheating and reaction initiation, and the pressure applied to the stack). Several important, and in some case unexpected, results were obtained. They include: (i) high chemical activity of the C–C composite, which allows the use of pure metals as the initial joining media; (ii) the importance of optimum P_f to be applied, because too low of a load does not provide good bonding, while too high of a P_f negatively affects the properties of the composite; (iii) the importance of the optimum value of the applied electrical current (i.e., too high a current causes the reactive media to melt and squeeze out of the stack before it can form a joint with good mechanical properties); and (iv) the final joined layer thickness appears to be independent of the thickness of the initial reactive layer. These and other results are described and discussed in detail below.

III. RESULTS AND DISCUSSION

In general, the joining process can be broken down physically into four stages (see also Fig. 3). The first is "inert preheating." During this stage, heat builds up in the sample due to resistance to the flow of electrical

current. The increase of temperature occurs primarily in the thin reactive layer because its resistivity is greater than in the bulk composite material. This continues until the ignition temperature of the reaction mixture is reached, which is typically close to the melting point of the least refractory component.[12] At this point, the second stage (i.e., the reaction) begins. In this approach, the reaction is uniformly initiated throughout the media volume, generating heat due to combustion and forming chemical bonds with the pieces to be joined. Once ignition has begun, the electrical current can be turned off. At some optimum time, the pressure applied to the joining stack is increased, which leads to densification of the reaction media, providing a joint with good mechanical properties (third stage). Finally, after the joining layer has been completely formed, the fourth stage, cooling, begins. A schematic representation of the joining stack structure on the first three stages is shown in Fig. 4.

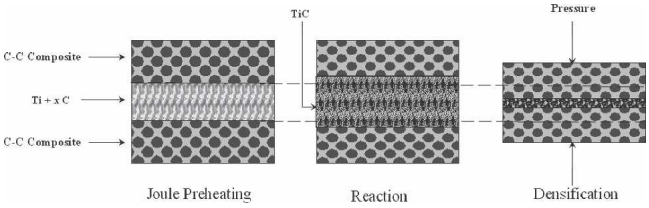

FIG. 4. Schematic representation of the interaction between composite and reactive media during the joining process.

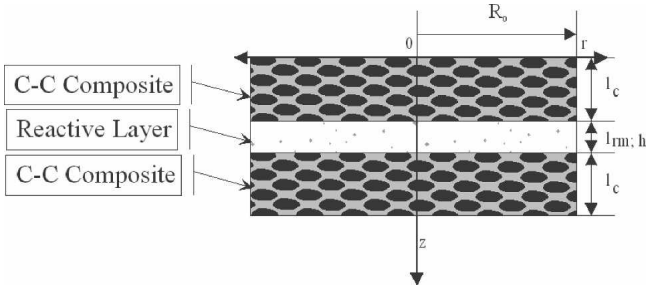

FIG. 5. Schematics of the joining stack.

A. Computer simulation of the preheating stage

Theoretical modeling was conducted to determine a range of parameters that could yield suitable conditions for joining C–C composites. It was assumed that the limiting stage in the joining process is the preheating of the reaction layer to the ignition temperature. That is, the Joule heating that takes place in the joining stack prior to reaction initiation. As mentioned above, for typical combustion systems the ignition temperature is about the melting point of the least refractory component (e.g., Ti in Ti–C and Ti–B mixtures). For example, the melting point of titanium (1933 K) can be taken as the temperature required to initiate the reaction in the reactive mixture layer.

In general, if electrical current (I) is passed through the solid sample (e.g., cylinder with radius R_0), the equation, which describes the temperature–time (T–t) history of the heating process, can be expressed as follows:

$$C_p\rho\frac{\partial T}{\partial t} = \lambda\frac{\partial^2 T}{\partial z^2} + \frac{I^2\phi(T)}{S^2} - \frac{2\sigma_0}{R_0}(T - T_0) - \frac{2\sigma F}{R_0}(T^4 - T_0^4) \quad , \tag{1}$$

where C_p, ρ, λ, and ϕ are the media heat capacity, density, thermal conductivity, and electrical resistivity, respectively, S is the sample cross-sectional area, σ_0 is a heat-transfer coefficient (loss to surroundings), σ is the Stefan–Boltzmann constant, F is a view factor, and T_0 is the ambient temperature.

Assume that the sample is a three-layer stack, consisting of two C–C composite disks (radius R_0 and thickness l_c) with a reactive layer (thickness l_{rm}) sandwiched between them (Fig. 5). The T–t history for Joule heating of such a stack can be defined by solving Eq. (1) with corresponding initial and boundary conditions (2):

$$t = 0; \quad T = T_0 \quad ,$$

$$z = 0; \quad T = T_0 \quad ,$$

$$z = l_c + l_{rm}/2; \quad \frac{\partial T}{\partial z} = 0 \quad . \tag{2}$$

Here, the boundary condition $T = T_0$ at $z = 0$ is chosen because: (i) the C–C disk is small compared to the massive copper electrode; and (ii) the duration of the process is very short (seconds). Moreover, in the scaled-up version of this apparatus, the electrodes are water-cooled. All of these factors provide conditions under which the change in temperature at the electrode ($z = 0$) is negligible.

The nonuniform physical characteristics of the stack are defined with the help of the error function to account for the changes in the material properties along the stack (i.e., composite–reaction mixture–composite) as follows:

$$C_p = C_{p,c} + \frac{1}{2}\cdot(C_{p,rm} - C_{p,c})\cdot\langle 1 + \mathrm{erf}\{10^5\cdot[h(z) - g]\}\rangle \quad ,$$

$$\rho = \rho_c + \frac{1}{2}\cdot(\rho_{rm} - \rho_c)\cdot\langle 1 + \mathrm{erf}\{10^5\cdot[h(z) - g]\}\rangle \quad ,$$

$$\lambda = \lambda_c + \frac{1}{2}\cdot(\lambda_{rm} - \lambda_c)\cdot\langle 1 + \mathrm{erf}\{10^5\cdot[h(z) - g]\}\rangle \quad ,$$

$$\phi = \phi_c + \frac{1}{2}\cdot(\phi_{rm} - \phi_c)\cdot\langle 1 + \mathrm{erf}\{10^5\cdot[h(z) - g]\}\rangle \quad ,$$

where

$$h(z) = \frac{z}{\left(1 + \frac{l_{rm}}{2 \cdot l_c}\right) l_c} = \frac{z}{\left(1 + \frac{1}{2 \cdot \gamma}\right) l_c} \quad ,$$

$$g = \frac{l_c}{\left(1 + \frac{l_{rm}}{2 \cdot l_c}\right) l_c} = \left(1 + \frac{1}{2}\gamma\right)^{-1} \quad ,$$

$$\gamma = \frac{l_c}{l_{rm}} \quad . \tag{3}$$

The parameters chosen in the error function ensure that the transition in the value of each physical characteristic is smooth and occurs as a step at the interface between the C–C composite and the reactive layer. The system of Eqs. (1)–(3), along with the experimentally defined physical properties of the joining materials (see Table I) was solved using the MATLAB (The MathWorks, Inc., Natick, MA) software package. Figure 6 indicates an example computed space–time–temperature distribution for a stack with $R_0 = 0.5$ cm, $l_c = 2.5$ cm, and $l_{rm} = 2$ mm using 600 A of current and $T_0 = 300$ K. As mentioned above (also see Table I), due to a high resistivity in the mixture, which is about an order of magnitude greater than that of the C–C composite, the temperature rises in the reactive layer more rapidly. It can be seen that the temperature in the reactive layer reaches the melting point of titanium in about 0.5 s, initiating the reaction and providing further heat generation and chemical interaction at the C–C composite surface interface. The ignition delay time (Δt_{ig}) depends on a variety of factors, such as current, initial temperature, and the stack dimensions.

TABLE I. Physical properties of materials used.

	Physical property			
Layer	λ (W/m-K)	ϕ (Ω-m)	ρ (kg/m^3)	C_p (J/kg-K)
Reactive layer	0.6	3×10^{-4}	1700	500
C–C composite	30	4.8×10^{-5}	1900	700

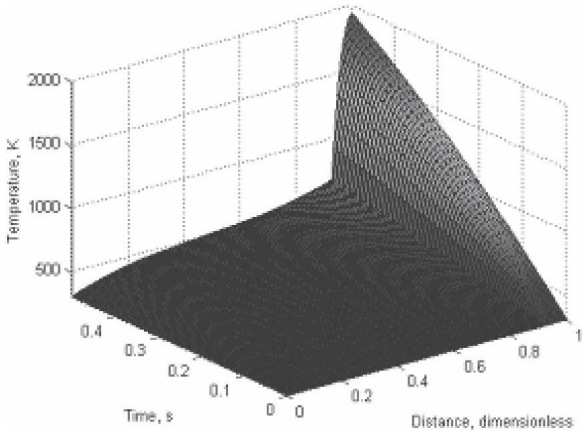

FIG. 6. Simulated time–temperature history in a laboratory-sized sample.

B. Optimization of the joining process

The influence of several parameters on the quality of the resulting joint was investigated. First, various compositions of reactive layer were used to join samples. Second, for each composition, three different values of current (600, 700, and 800 A) were used to initiate the reaction. Finally, the effect of the applied P_f was investigated. The comparative quality of the joint was determined with a tensile strength test.

1. Reaction mixture composition

Different exothermic mixtures, including, for example, Ti–C, Ti–B, Ti–B–C, and Ti–C–Ni, were used in the joining layer. These systems were selected based on their high exothermicity. For example, the adiabatic combustion temperatures (T_{ad}) for Ti + B, Ti + C, and 3Ti + B + C compositions are 3348, 3290, and 2600 K, respectively. However, it was found that the exothermicity of the reaction layer is not indicative of the quality of the joint. Some results for joints obtained under otherwise similar experimental conditions ($I = 600$ A, $P_i = 3.5$ MPa, $P_f = 51$ MPa, $\Delta t_l = 1$ s, $\Delta t_h = 5$ s), but different reaction mixture compositions are shown in Table II. It can be seen that there is no clear correlation between T_{ad} and the mechanical properties of the joint.

Moreover, it looks like the system with the lowest T_{ad} possesses the highest σ_{TS}. This effect is illustrated even more clearly in Fig. 7, which shows that a reaction mixture (Ti + 8 wt% Ni) with almost zero exothermicity ($T_{ad} \sim 560$ K) results in a joint with the highest tensile strength.

Investigation of the microstructure of the joining layer allows one to solve this "puzzle." Figure 8 shows a typical cross section of the joined stack, obtained by using a 2-mm disk of pure titanium powder as the "reaction mixture" layer. First, it can be seen that the joining layer is very thin (~10 μm) and uniform. Second, no microcracks can be observed along the C–C composite-layer

TABLE II. Mechanical properties of joints obtained for different reactive mixtures.

System	Tensile strength (MPa)	Square root deviation (MPa)	Adiabatic combustion T (K)
Ti + 0.1C + 8 wt% Ni	5.5	0.9	1041
Ti + 0.5C + 8 wt% Ni	3.1	0.9	2114
Ti + 0.5C	2.0	0.7	2217
3Ti + B + C	1.8	0.6	2600
T + B	2.1	0.7	3348

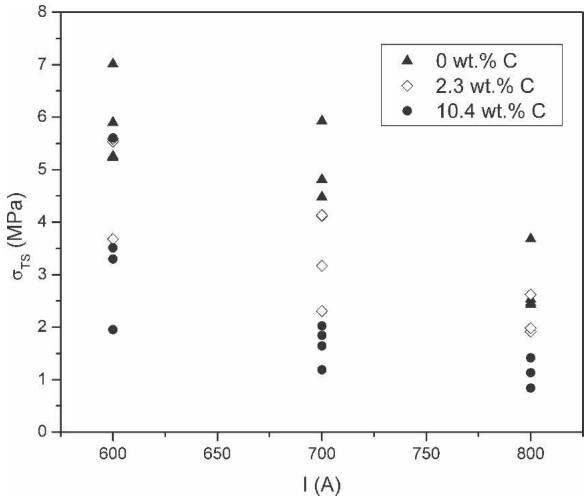

FIG. 7. Comparison of tensile strength for samples joined with different Ti + xC + 8 wt% Ni mixtures.

interfaces regardless of whether they were carbon fiber/layer or CVD–carbon/layer surfaces. More importantly, energy dispersive spectroscopy (EDS) analysis proves that the layer is composed of stoichiometric titanium carbide. Table III summarizes the results of EDS analysis performed at the points indicated in Fig. 8. It is also important to note that the concentration of titanium gradually decreases over a distance of about 10 μm into the composite from the joint layer.

Thus, a refractory layer ($T_{mp,TiC}$ ~ 3290 K) was formed as a result of the chemical reaction between the titanium melt and carbon from the C–C composite. As a result, when there are fewer nonmetal reactive components (e.g., C or B) present in the initial mixture, more carbon from the composite material participates in the reaction, providing a better joint. Also, when C or B powders are present in the reaction mixture, they rapidly react with Ti, causing a significant increase in matter viscosity, simultaneously lowering mass transport in the layer. These effects also result in weaker chemical bonding between the joint layer and composite. This finding led to the general idea of using the components that are to be "welded" (e.g., C–C composite) as reactive elements, interacting with the joining layer components (e.g., Ti) to produce a refractory joint layer.

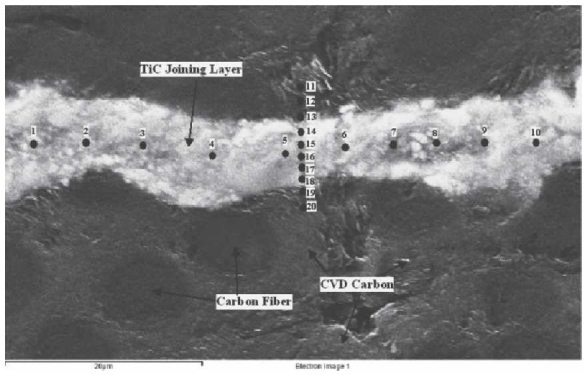

FIG. 8. Typical microstructure of a joined C–C composite sample (adapted from White et al.[22]).

Further experiments show that the mechanical properties of the joint increase if some amount of nickel (~8 wt%) is added to the titanium powder. This effect can be explained because the nickel matrix allows for much better bonding between refractory titanium carbide grains. Also, it was demonstrated that instead of titanium powder, one could use a thin (e.g., 25 μm) Ti foil to produce good bonding between C–C composite pieces (see Fig. 9). As such, components with a complex shape can be joined. It is also interesting that the thickness of the final joint layer is essentially independent of the initial thickness; this effect is discussed later.

2. Influence of electrical current magnitude

On one hand, it was proven that for the investigated systems, the joining of the C–C samples with significant strength did not occur when current <600 A was used. On the other hand, the results shown in Figs. 7 and 9 reveal that, in general, the tensile strength of the joint decreases as the magnitude of the current is increased.

Estimations based on the data presented in Table I, as well as on experiments, show that for the investigated conditions, current <600 A does not provide stack heating up to the melting point of Ti. This fact explains the existence of a critical current value of I_{cr} = 600 A. It is more difficult to understand why the mechanical properties of the joint decrease with increasing electrical current above I_{cr}. Again, investigation of the microstructure of the obtained stacks allows clarification of this issue. The

TABLE III. Elemental distributions along and normal to the joint layer.

Direction relative to joint layer	Distribution									
Along										
Position of EDS analysis	1	2	3	4	5	6	7	8	9	10
Ti/C concentration (wt%)	76.9/23.1	78.5/21.5	76.7/23.3	80.9/19.1	78.5/21.5	65.5/34.5	73.7/26.3	68.2/31.8	76.0/24.0	76.3/23.7
Normal										
Position of EDS analysis	11	12	13	14	15	16	17	18	19	20
Ti/C concentration	9.0/91.0	26.9/73.1	58.7/41.3	76.2/23.8	79.5/20.5	81.3/18.7	73.0/27.0	41.4/58.6	21.3/78.7	8.2/91.8

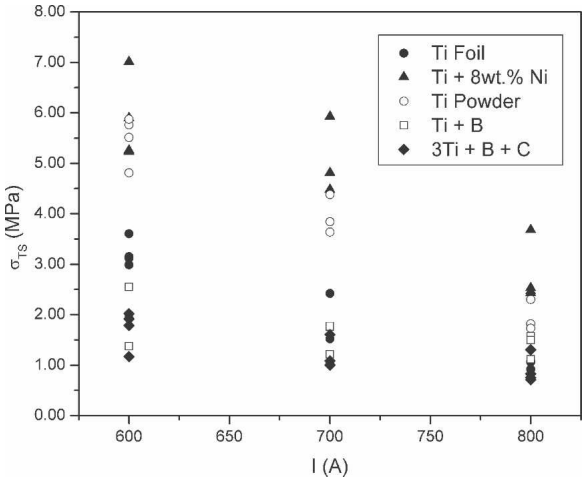

FIG. 9. Comparison of tensile strength for samples joined under different heating conditions.

typical microstructure of the joining layer obtained at high current (800 A) is presented in Fig. 10. It is clear that there is no continuous joint layer formed under such conditions. The high-magnification insert demonstrates that some chemical interaction between titanium and carbon occurred; however, the extent of the titanium carbide phase is not enough to form a continuous layer. Thus, it can be suggested that higher electrical current, which creates a higher temperature in the joining layer, results in very rapid squeezing of liquid metal from the gap. This lack of sufficient reagent does not allow the development of good bonding between the joining pieces.

3. Influence of maximum applied pressure

In all of the previous investigations, the lower amperage (600 A) condition yielded the best results, so it was used along with the Ti + 8 wt% Ni composition. The maximum pressure applied to the stack, at $\Delta t_1 = 1.0$ s after beginning the preheating stage, was varied between 3.5 MPa (the initial pressure) and 51 MPa. This resulted in some interesting findings. It was found that when a relatively low pressure was applied to the stack during joining, the joined components would fail along the joint when submitted to a tensile stress. However, above some critical value, it appears that the joined samples began failing in the composite material away from the area where they were joined. This is shown in the tensile strength results of Fig. 11. Another conclusion from this round of experiments is that it appears it is not advantageous to apply a pressure greater than this critical value. While the samples still failed away from the joint, the magnitude of the tensile strength decreased. This effect is related to the influence of the process conditions on the mechanical properties of the C–C composite material. Additional experiments confirmed that application of high compressive loads followed by rapid unloading leads to C–C composite exfoliation.

C. Joining mechanism

To understand the joining mechanism further, let us first look at the diffusion of carbon into the liquid titanium melt. Using the Stokes–Einstein relation [Eq. (4)], the diffusion coefficient for C in Ti at the melting point of Ti can be approximated:

$$D_{\mathrm{m}} = \frac{k_{\mathrm{B}} T_{\mathrm{m}}}{4\pi\mu r_{\mathrm{c}}} \quad , \tag{4}$$

where D_{m} is the diffusion coefficient of the solid (e.g., C) in the liquid (e.g., Ti), k_{B} is the Boltzmann constant, T_{m} is the melting point of the liquid, μ is the viscosity of the liquid, and r_{c} is the radius of the diffusing particle. For this system, titanium has a viscosity on the order of 10^{-3} Pa-s,[24] and the radius of carbon is about 0.7 Å, resulting in a diffusion coefficient on the order of $D_{\mathrm{m}} \sim 10^{-5}$ cm^2/s.[25] The duration (Δt_r; reaction time) of

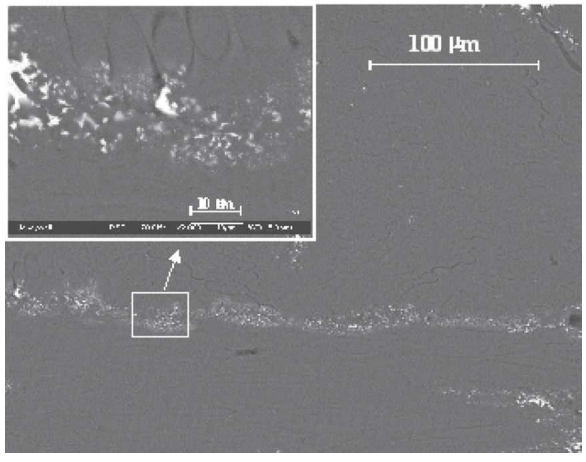

FIG. 10. Microstructure of the joint layer formed under high electric current (800 A).

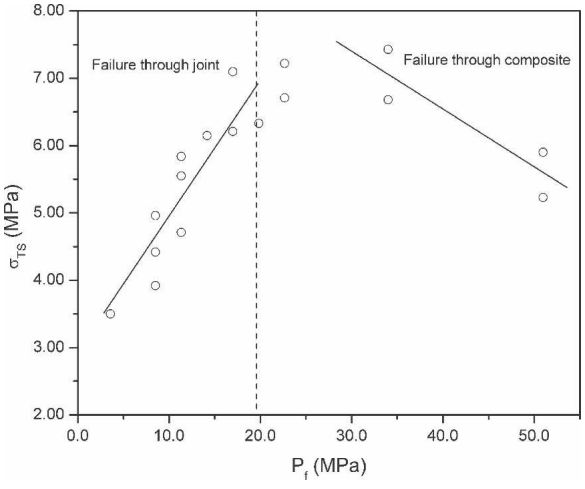

FIG. 11. Comparison of tensile strength for samples joined with a Ti + 8 wt% Ni mixture.

the joining process during which a high-temperature region ($T > T_{m.p.,Ti} = 1993$ K) existed was at least 1 s. Using this, one can estimate the diffusion length as follows:

$$l_d \sim \sqrt{D_m \Delta t_r} \sim 30\ \mu m \quad . \tag{5}$$

This value exceeds the final thickness ($\Delta_f \sim 10$ μm) of the obtained joining layer (see Fig. 8) under optimum bonding conditions ($I_{max} = 600$ A, $P_f = 20$ MPa) (Fig. 11). Also, it was shown that the Δ_f of the joining layer was essentially independent of the initial reactive media thickness. Indeed, Δ_f was ~10 μm when either a 2-mm disk compacted from Ti powder or a 25-μm Ti foil was used as a reactive layer. All these results suggest that in addition to chemical interaction between carbon and liquid metal, the process of liquid flow in the gap under applied pressure plays an important role in the formation of the joint.

To estimate the characteristic squeezing rate of melts in the gap, let us modify a solution obtained in the study by Landau and Lifshitz[26] for liquid flow between two parallel round plates with radius R_0, one of which is fixed and the other one moves with constant velocity (U) toward the other. It was shown that in this case the radial velocity of liquid flow (v_r), pressure (p), and force (F) acting on the plate can be calculated as follows:

$$v_r = \frac{1}{2\eta}\cdot\frac{dp}{dr}\, z(z-h) \quad ,$$

$$p = p_0 + \frac{3\eta U}{h^3}(R_0^2 - r^2) \quad ,$$

$$F = \frac{3\pi\eta U R_0^4}{2h^3} \quad , \tag{6}$$

where η is the dynamic viscosity of the melt, h is the instantaneous distance between the plates, and p_0 is the atmospheric pressure. These relations obtained for a quasistationary approximation are correct in the case when a constant load (F) is applied to the plate. In such a case, the velocity of plate movement can be estimated as

$$U = \frac{2F}{3\pi\eta R_0^4} h^3 \quad . \tag{7}$$

The complex metal–carbide melt in the joining layer is a liquid with high viscosity, and thus the quasistationary approximation can be applied to the considered conditions. If one neglects the process of liquid solidification (due to heat losses, as well as crystallization of the refractory product), the velocity with which the plates approach each other when constant pressure, P, is applied to the lower plate can be calculated as follows:

$$U = -\frac{dh}{dt} = -\frac{2F}{3\pi\eta R_0^4} h^3$$
$$= -\frac{2}{3\eta}\cdot\frac{F}{\pi R_0^2}\cdot\left(\frac{h_0}{R_0}\right)^2\cdot\frac{h^3}{h_0^2} = -\left[\frac{2P}{3\eta}\cdot\left(\frac{h_0}{R_0}\right)^2\right]\cdot\frac{h^3}{h_0^2}$$
$$= B\cdot\frac{h^3}{h_0^2} \quad . \tag{8}$$

Integrating Eq. (8) with initial condition $h(t = 0) = h_0$ gives the relation for the instantaneous thickness of the reactive layer (h), which becomes liquid upon reaching the melting point of titanium:

$$h = \frac{h_0}{\sqrt{1 + 2Bt}}$$
$$= \frac{h_0}{\sqrt{1 + t/t_f}} \quad , \tag{9}$$

where t_f, the characteristic squeezing time, is defined as

$$t_f = \frac{3\eta}{4P}\cdot\left(\frac{R_0}{h_0}\right)^2 \quad . \tag{10}$$

For a sample with $R_0 = 0.5$ cm, an initial thickness of $h_0 = 4$ mm, an applied pressure of $P = 3.5$ MPa (the initial load used), and a viscosity of $\eta = 5 \times 10^{-3}$ Pa-s for liquid titanium at its melting point, Eq. (10) shows that the layer is squeezed to the micron scale in a time period on the order of 0.1 s (see Fig. 12). We believe that it is not mere coincidence that the carbon diffusion length for $\Delta t_r = 0.1$ s estimated using Eq. (5) is ~10 μm.

Frame-by-frame analysis of video recordings of the joining process enables the determination of the experimental dependence $h = h(t)$. An example using 600 A of

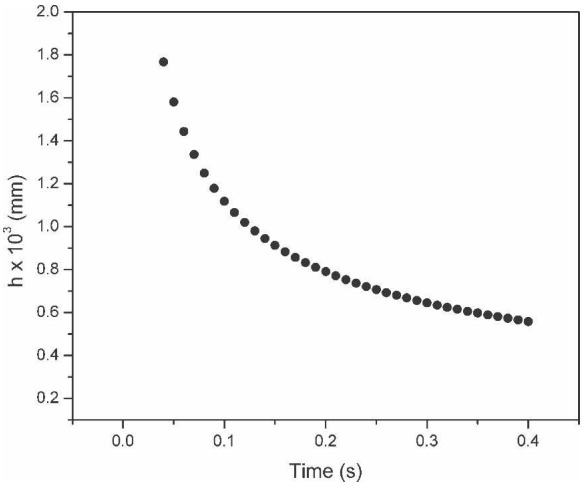

FIG. 12. Squeezing of a melted titanium layer between two plates using Eq. (9).

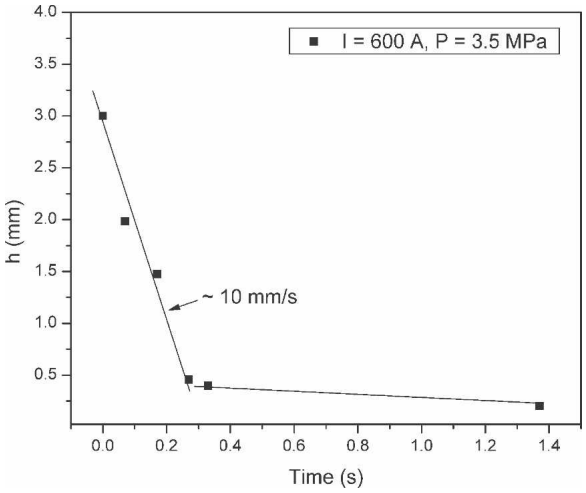

FIG. 13. Experimental data on the change in distance between two C–C cylinders during the joining process.

current and conditions similar to those used for the theoretical calculations is shown in Fig. 13. It can be seen that, indeed, on the initial stage (~0.2 s) the gap decreases rapidly (~10 mm/s), while the squeezing slows once the distance is <500 μm. These results are in good qualitative agreement with theoretical predictions.

The above estimations suggest the following physical model for the joining process. Upon Joule heating, temperature in the titanium layer rapidly rises until it reaches its melting point (1993 K). Even under relatively low initial pressure (P_i = 3.5 MPa), the melted titanium is rapidly squeezed out of the gap between the pieces to be joined. Simultaneously, carbon from the composite material is dissolved into the liquid-metal layer, leading to the formation of a refractory phase (TiC) with a much higher viscosity than the metal. Because the characteristic squeezing rate is much higher than the characteristic diffusion time, the thickness of the final joining layer is essentially independent of h_0. It is important for the composite material to chemically bond with the joining layer to form a good joint. The addition of C to the reactive layer (i.e., Ti + xC mixture) decreases the diffusion rate of carbon from the composite material, which results in diminished chemical interaction between the layer and the pieces to be welded. Hence, the strength of the formed joint is reduced.

IV. CONCLUSIONS

Our design has proven the RRW approach is effective for joining C–C composites that are used for carbon brakes. In fact, joints that possess higher mechanical properties than the composite itself have been achieved. Additionally, several other results were found: (1) the C–C composite possesses a high enough activity that supplemental carbon in the reactive media is not needed; (2) increasing the pressure beyond a critical value can negatively affect the composite itself; (3) using too much electrical current appears to cause the reactive media to melt and squeeze out before it can form a joint with good mechanical properties; and (4) the final joined layer thickness was independent of the thickness of the initial reactive media. Though some of these results are surprising, they have shown that the process is even more viable than originally thought. Plans are currently under way to scale the operation for use in an industrial environment.

ACKNOWLEDGMENTS

The Indiana 21st Century Research and Technology Fund has supported this work. The authors would like to thank Dr. Edmundo Corona for his consultation and the use of the solid-mechanics testing facility.

REFERENCES

1. U. Rieck, J. Bolz, and D. Mullerkliesner: Advanced materials for space applications. *Int. J. Mater. Prod. Tec.* **10,** 303 (1995).
2. C. Byrne: Modern carbon composite brake materials. *J. Compos. Mater.* **38,** 1837 (2004).
3. A.H. Simpson, S.T. Fryska, M.L. LaForest, and B.P. Soos: Formulation for the manufacture of carbon-carbon composite materials. U.S. Patent Application No. 20060073338, 2006.
4. A.S. Mukasyan and J.D.E. White: Combustion joining of refractory materials, in *Combustion of Heterogenous Systems: Fundamentals and Applications for Materials Synthesis,* edited by A.S. Mukasyan and K.S. Martirosyan (Transworld Research Network, Kerala, India, 2007), pp. 219–245.
5. P. Dadras and G.M. Mehrotra: Solid-state diffusion bonding of carbon-carbon composites with borides and carbides. *J. Am. Ceram. Soc.* **76,** 1274 (1993).
6. P. Dadras and G.M. Mehrotra: Joining of carbon-carbon composites by graphite formation. *J. Am. Ceram. Soc.* **77,** 1419 (1994).
7. P. Dadras, T.T. Ngai, and G.M. Mehrota: Joining of carbon-carbon composites using boron and titanium disilicide interlayers. *J. Am. Ceram. Soc.* **80,** 125 (1997).
8. L.A. Xue and D. Narasimhan: Joining of rough carbon–carbon composites with high joint strength. U.S. Patent No. 5 972 157, October 26, 1999.
9. L.A. Xue and D. Narasimhan: Joining of rough carbon–carbon composites with high joint strength. U.S. Patent No. 6 174 605 B1, January 16, 2001.
10. Z.A. Munir and U. Anselmi-Tamburini: Self-propagating exothermic reactions: The synthesis of high-temperature materials by combustion. *Mater. Sci. Rep.* **3,** 277 (1989).
11. J.J. Moore and H.J. Feng: Combustion synthesis of advanced materials: 2. Classification, applications and modeling. *Prog. Mater. Sci.* **39,** 275 (1995).
12. A. Varma, A.S. Rogachev, A.S. Mukasyan, and S. Hwang: Combustion synthesis of advanced materials: Principles and applications. *Adv. Chem. Eng.* **24,** 79 (1998).
13. Y. Miyamoto, T. Nakamoto, M. Koizumi, and O. Yamada: Ceramic-to-metal welding by a pressurized combustion reaction. *J. Mater. Res.* **1,** 7 (1986).
14. V.A. Shcherbakov and A.S. Shteinberg: SHS welding of refractory materials. *Int. J. Self-Propag. High-Temp. Synth.* **2,** 357 (1993).

15. R.W. Messler and T.T. Orling: Joining by SHS. *Adv. Powder Metall. Part. Mater.* **6,** 273 (1994).
16. K. Uenishi, H. Sumi, and K.F. Kobayashi: Joining of the intermetallic compound TiAl using self-propagating high-temperature synthesis reaction. *Z. Metallkd.* **86,** 64 (1995).
17. K. Matsuura, M. Kudoh, J.H. Oh, S. Kirihara, and Y. Miyamoto: Development of freeform fabrication of intermetallic compounds. *Scripta Mater.* **44,** 539 (2001).
18. C. Pascal, R.M. Marin-Ayral, and J.C. Tedenac: Joining of nickel monoaluminide to a superalloy substrate by high pressure self-propagating high-temperature synthesis. *J. Alloys Compd.* **337,** 221 (2002).
19. V.A. Shcherbakov: SHS welding of hard alloy and steel. *Key Eng. Mater.* **217,** 215 (2002).
20. A.S. Shteinberg, A.G. Merzhanov, I.P. Borovinskaya, O.A. Kochetov, V.B. Ulibin, and V.V. Shipov: U.S.S.R. Patent No. 747661, Buleten Izobretenii, 1980.
21. J. Wang, E. Besnoin, A. Duckham, S.J. Spey, M.E. Reiss, O.M. Knio, and T.P. Weihs: Joining of stainless-steel specimens with nanostructured Al/Ni foils. *J. Appl. Phys.* **95,** 248 (2004).
22. J.D.E. White, A.S. Mukasyan, M.L. La Forest, and A.H. Simpson: Novel apparatus for joining of carbon-carbon composites. *Rev. Sci. Instrum.* **78,** 015105 (2007).
23. Z.A. Munir, U. Anselmi-Tamburini, and M. Ohyanagi: The effect of electric field and pressure on the synthesis and consolidation of materials: A review of the spark plasma sintering method. *J. Mater. Sci.* **41,** 763 (2006).
24. T. Iida and R.I.L. Guthrie: *The Physical Properties of Liquid Metals* (Oxford University Press, Oxford, England, 1988), p. 288.
25. A.S. Shteinberg and V.A. Knyazik: Macrokinetics of high-temperature heterogeneous reactions: SHS aspects. *Pure Appl. Chem.* **64,** 965 (1992).
26. L.D. Landau and E.M. Lifshitz: *Fluid Mechanics*, 2 ed. (Pergamon Press, Oxford, England, 1987), p. 539.